HHS Public Access

Author manuscript

J Biophotonics. Author manuscript; available in PMC 2023 November 01.

Published in final edited form as:

J Biophotonics. 2022 November ; 15(11): e202200052. doi:10.1002/jbio.202200052.

OCT Evaluation of Vaginal Epithelial Thickness during CO_2 Laser Treatment: A Pilot Study

Yusi Miao[1,2,†], **Neha T Sudol**[3,†], **Yan Li**[1,2], **Jason J Chen**[1,2], **Rebecca A. Arthur**[3], **Saijun Qiu**[1,2], **Yuchen Jiang**[1,2], **Yona Tadir**[1], **Felicia Lane**[3], **Zhongping Chen**[1,2,*]

[1]Beckman Laser Institute & Medical Clinic, University of California, Irvine, Irvine, CA, USA

[2]Department of Biomedical Engineering, University of California, Irvine, Irvine, CA, USA

[3]Department of Obstetrics & Gynecology, University of California, Irvine, Medical Center, Irvine, CA, USA

Abstract

Genitourinary syndrome of menopause (GSM) negatively affects more than half of postmenopausal women. Energy-based therapy has been explored as a minimally invasive treatment for GSM; however, its mechanism of action and efficacy is controversial. Here, we report on a pilot imaging study conducted on a small group of menopause patients undergoing laser treatment. Intravaginal optical coherence tomography (OCT) endoscope was used to quantitatively monitor the changes in the vaginal epithelial thickness (VET) during fractional-pixel CO_2 laser treatment. 11 patients with natural menopause and 1 surgically induced menopause patient were recruited in this clinical study. Following the laser treatment, the 6 out of 11 natural menopause patient showed increase in both proximal and distal VET, while 2 natural menopause patient showed increase in VET in only one side of vaginal tract. Furthermore, the patient group that showed increased VET had thinner baseline VET compared to the patients that showed decrease in VET after laser treatment. These results demonstrate the potential utility of intravaginal OCT endoscope in evaluating the vaginal tissue integrity and tailoring vaginal laser treatment on a per-person basis, with the potential to monitor other treatment procedures.

Graphical Abstract

*Correspondence: Zhongping Chen, Department of Biomedical Engineering, University of California, Irvine, Irvine, CA, USA, z2chen@uci.edu.

†Y.M. and N.T.S have contributed equally to this work.

AUTHOR CONTRIBUTIONS

Y.M., N.S., and J.C. contributed to the conception and design of the work. Y.M., N.S., Y.L., S.Q., Y.J., and R. A. acquired the data. Y.M. and J.J. conducted the analyses, prepared figures, and interpreted the results. F.L. and Z.C. supervised the study. Y.M., N.S., J.C., Y.T., and F.L. contributed to the drafting of the manuscript. Z.C. accepts responsibility for the integrity of the data analyzed.

CONFLICT OF INTEREST

Y.M., Y.L., Y.T., and Z.C. have an unlicensed patent application (US20190200851A1) on the use of intravaginal OCT as a diagnostic technology in GSM. Y.T. is a consultant for Alma Laser. N.S., J.C., R.A., S.Q., Y.J. and F.L. declare no potential conflict of interest.

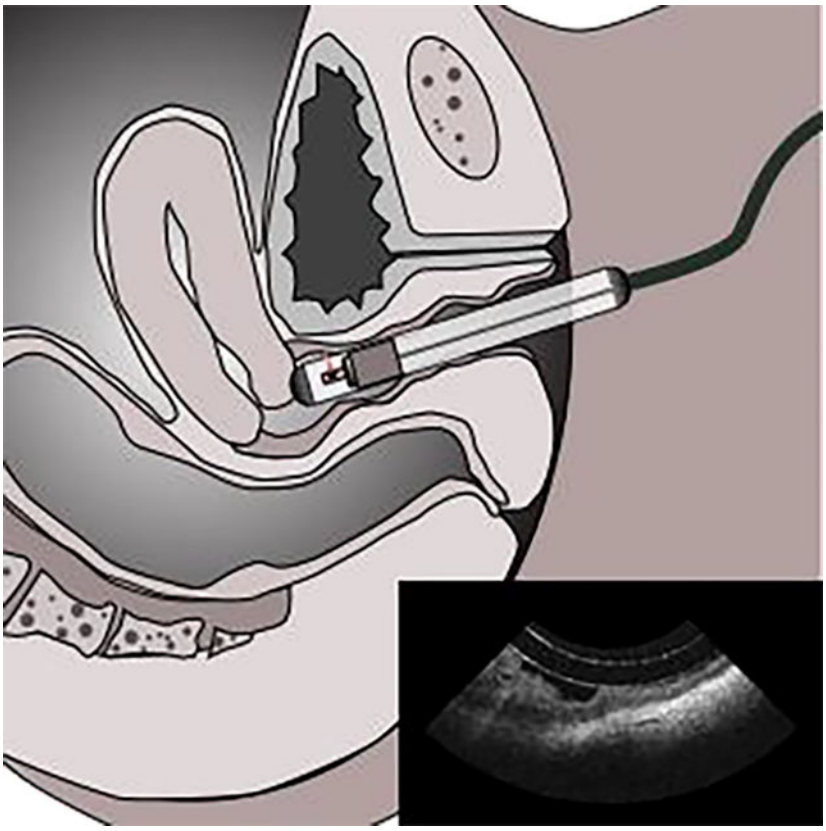

Genitourinary syndrome of menopause (GSM) negatively affects more than half of postmenopausal women. Energy-based therapy has been explored as a minimally invasive treatment for GSM; however, its mechanism of action and efficacy is controversial. Here, we report on a pilot imaging study conducted on a small group of menopause patients undergoing laser treatment. Intravaginal OCT endoscope was used to quantitatively monitor the changes in the vaginal epithelial thickness (VET) during fractional-pixel CO_2 laser treatment. The results demonstrate the potential utility of intravaginal OCT endoscope in evaluating the vaginal tissue integrity and tailoring vaginal laser treatment.

Keywords

endoscope; clinical research; genitourinary syndrome of menopause; laser therapy; optical imaging; rejuvenation

1 INTRODUCTION

Genitourinary syndrome of menopause (GSM) is a broad medical term describing a variety of symptoms—including vulvovaginal atrophy, dryness, burning, itching, urinary disorders, and more—that arises from a decline in estrogen levels [1–3]. Although it is not a life-threatening condition, GSM has a negative impact on a woman's quality of life with regards to general health and sexual function [4]. Hormone therapy is commonly used to supplement the body's natural estrogen and relieve menopause symptoms [5]. However,

safety concerns associated with long-term hormone therapy exists, including the increased risk of blood clots, breast cancer, and endometrial cancer [6–8]. Due to these safety concerns and even the efficacy of long-term use of topical or systemic hormone therapy as the conventional treatment, an increasing number of women are now seeking more modern approaches. One contemporary method that is not yet FDA approved for treating GSM is the use of energy-based devices, such as a fractional laser [9–11]. This tool stimulates vaginal tissue regeneration to improves the physiological condition of the tissue [12,13]. Limited pathology evidence from human studies has demonstrated an increase in vaginal epithelial thickness (VET), vascularization in lamina propria, re-collagenation, and elastin formation in the genitourinary tract due to the thermally induced healing process [12–14]. Although conventional histology data obtainable from biopsy can provide information of tissue histopathology, it is rarely performed on vaginal tissue because of its invasive nature. Therefore, the capability to demonstrate clinically significant histology comparing treatment-related vaginal tissue changes is of high scientific and clinical value as it can provide histopathological information before and over the time course of therapy to monitor and optimize the treatment.

Several techniques have been proposed to non-invasively assess tissue structures and vasculatures in the female reproductive system. Transvaginal ultrasound is helpful in evaluating macrostructures like the uterus and ovaries. However, ultrasound imaging cannot accurately assess VET and underlying microstructures since the spatial resolution of ultrasound is limited to 50 – 200 μm [15,16]. In the recent report, a transvaginal photoacoustic endoscopy was presented for *in vivo* imaging of capillary network in human cervix [17]. While photoacoustic imaging (PAI) combines ultrasound and optical imaging to achieve high resolution deep tissue imaging, this technique is mainly used for vascular imaging as the contrast of PAI relies on the optical absorption. Optical coherence tomography (OCT), on the other hand, can provide high-resolution, 3D, non-invasive tissue scanning similar to ultrasound but with micron-scale resolution [18,19]. Using non-ionizing near-infrared light, OCT can visualize depth-resolved information in three-dimension *in vivo* with a spatial resolution 2–3 order of magnitude higher than that of ultrasound imaging and PAI. With high spatial resolution attainable by OCT and low-coherence interferometry, several groups have reported the accurate depth measurement of vaginal tissue layers and gel coating applied on top [20–24]. Most recently, Xu et al. conducted an extensive clinical study with a total of 63 patients to evaluate the clinical efficacy of OCT in detecting vulvar diseases, concluding high accuracy of OCT examination compared to pathological results [25]. Another recent study by Moiseev et al. explored the ability of OCT to visualize lymphatic vessels from vulva tissue [26]. In addition to the direct visualization of tissue morphology and vascular features, several studies have also implemented OCT in monitoring drug response in vaginal tissue [27,28]. Vincent *et al.* have previously validated VET measurements after treated with nonoxynol-9, a spermicide that causes epithelial disruption and thinning, in sheep [27,28]; they demonstrated the capability of OCT to visualize the epithelial-lamina propria interface and VET changes. Nevertheless, the forward-viewing catheter-based OCT imaging system employed by many of the previous studies was limiting in imaging speed and scan area, which make it impossible to visualize the entire volume of vaginal canal. In the recent studies, we developed an OCT imaging

catheter with wide-field scanning capability for intravaginal tissue imaging in the human vaginal canal *in vivo* [29,30]. However, the small form factor of the thin imaging catheter (outer diameter of 1.2 mm) used by Yan et al. [29], while providing the benefit of minimal discomfort, cannot allow for comprehensive assessment of the human vaginal structure due to its highly folding nature. The oblong-shape imaging probe (outer diameter of 12 mm) was introduced in the successive clinical study [30] to resolve the issues of vaginal folding during imaging and to provide more accurate measurement of the vaginal epithelial thickness. In the present study, we adopted the similar oblong-shape intravaginal probe to investigate the effects of laser treatment on vaginal tissue.

Here, we present an OCT-based approach to objectively and accurately quantify VET throughout the entire vaginal canal *in vivo*. We employed a handheld intravaginal OCT probe to capture the full volume of human vagina in high resolution, and this enabled us to study the effect of vaginal laser therapy based on VET measurements obtained before and after the laser treatment. To complement the large number of images obtained through volumetric imaging, we applied a deep learning technique to segment the vaginal epithelium for high-throughput VET measurement and vaginal reconstruction in 3D. The novelty of this pilot study compared to the previous human OCT studies [29,30] is as follow: we 1) demonstrated an endoscopic imaging and analysis approach to extract and reconstruct epithelial layer across entire vaginal tract, 2) investigated the effect of laser therapy on VET through a larger sample size compared to the previous study [30], 3) analyzed the spatial variation of VET changes, and 4) assessed the dependency of baseline VET on the laser treatment effects.

2 MATERIALS AND METHODS

2.1 Intravaginal OCT endoscopy system

The OCT imaging system is based on a typical 1.3 μm swept-source OCT system with a 100 kHz vertical-cavity surface-emitting laser (SL1310V1-10048, Thorlabs Inc., NJ), similar to what we have described in our previously studies [29,30]. The axial resolution of our OCT system is about 8 μm in tissue. For *in vivo* imaging of the full vaginal canal, we designed a handheld intravaginal endoscope based on the catheter-type endoscope [29,31] as shown in Figure 1. To accommodate for the highly elastic property of vaginal canal and to minimize vaginal folding, in this study, we designed a clear oblong-shape outer protective cover with an outer diameter of 12 mm and a length of 150 mm. To acquire a concentric scanning of the endoscope, we designed a centerpiece consists of a rotational bearing and a 3D printed support. The centerpiece can also slide across the oblong-shape cover so that full vaginal canal scanning can be obtained. In this study, the endoscope was rotated at 3,000 revolutions per minute driven by an external rotary junction (MJP-SAP-131, Princetel Inc., NJ). Volumetric OCT scanning of the entire vagina was obtained by withdrawing the probe at a constant speed of approximately 0.5 mm/s. The full scan of vaginal scan was completed approximately in 40 seconds.

2.2 Fractional CO_2 laser treatment protocol

Participants underwent three intravaginal treatments at 4–6 weeks intervals with the fractional-pixel CO_2 laser system (FemiLiftTM, Alma Lasers, Israel). The laser beam is fractionated into 81 microbeams (pixels) at each activation (per 1 cm^2) and the laser intensity allows an adjustment to the patient's tolerance, ranging from 40–120 mJ/pixel. The procedure was repeated two times at each session. The setting used in this study: was 50–100mJ/pixel based on each patient's comfort level. The laser beam was applied with a vaginal probe, gently inserted up to the top of the vagina and subsequently withdrawn at 1-cm intervals while rotated to four positions in each station to provide complete circumferential treatment of the vagina. Local anesthetic cream was applied to the introitus for 10 minutes and wiped clean and dried before vaginal laser therapy. Participants were advised to avoid sexual activity for at least 3 days after each laser application.

2.3 Imaging protocol for human subjects

A total of 12 postmenopausal women were recruited in this study. All studies were done under the approval of the UC Irvine institutional review board (IRB). Imaging was conducted in accordance with guidelines set forth in protocol number 2017–3686 and with individual informed patient consent. All subjects reported moderate-to-severe GSM symptoms and received one-time pixelated fractional CO_2 laser treatment using a commercial device (FemiLift, Alma Lasers Inc., IL). Intravaginal OCT imaging was performed before as well as 4 – 6 weeks after the laser treatment to assess the treatment effects on the vaginal canal histopathology. All participants were imaged in a standard gynecologic examination room. The patients were positioned in dorsal lithotomy during OCT imaging. A small amount of water-based vaginal lubricant was applied to the surface of the protective cover of the imaging probe before the clinician maneuvered the intravaginal probe into the vagina opening. The distal tip of the imaging probe was navigated to the cervix for obtaining the full volume of the vaginal canal. Once positioned, an operator initiated the probe rotation and translation within the protective cover to acquire the data. Scanning of the entire vaginal canal was completed within approximately 40 seconds. The patients reported only minimal discomfort from the insertion of the protective cover and the motion caused by the rotating probe.

2.4 Segmentation and quantitative analysis

We extracted the VET from the OCT images using a semi-automated segmentation method. In the vaginal OCT images, VET represents the dark layer between strongly reflecting the mucus layer and lamina propria. To facilitate the segmentation process, we first applied a deep learning segmentation algorithm based on U-Net to locate and extract the VET [32,33]. To train the U-NET model, 200 OCT images were selected from four 3D OCT data sets and the VET was manually labeled by an experienced OCT reader. Among all the labeled images, 40 images were used to evaluate the accuracy of the model and 160 images were used to train the model. Dice similarity coefficient below is used to evaluate the training accuracy. Dice similarity coefficient was used to evaluate the training accuracy, which can be calculated as $2|X \cap Y| / (|X| \cup |Y|)$, where X is prediction and Y is ground truth (manual label). In this research, the resulting Dice coefficient was 0.775. Then, the final output of the

deep learning segmentation was manually examined and compensated by a human reader to increase the accuracy of VET analysis.

2.3 Statistical Analysis

Statistical analyses were performed using R (version 3.5.1). Arithmetic mean was compared using Wilcovon-Mann-Whitney test after the differences in the variances were tested. P values of less than 0.05 were considered statistically significant.

3 RESULTS

3.1 Vaginal OCT patient imaging and 3D reconstruction

OCT images were acquired and analyzed from patient 1 in Table 1 to demonstrate the processing pipeline. The *in vivo* OCT images demonstrate an imaging depth of approximately 1.5 mm into the vaginal wall and can resolve the mucus, epithelium, lamina propria, and venous plexuses (Figure 2). The epithelium layer had lower pixel intensity due to its less scattering optical property with respect to the mucus and lamina propria. The boarders between the mucus and the epithelium, as well as between the epithelium and the lamina propria were well-demarcated and easily differentiated visually by clinicians. As opposed to our previous study [29], the protective cover that slightly extends the vaginal wall allows for imaging of more surface area, and thus revealed the heterogeneity of vaginal epithelium including rete ridges. Generally, the distal region of the vagina had thicker epithelium and more vaginal folds. From the OCT scan across vaginal tract, the extent of folds appears to continue to increase until eventually reaching lamina minora (not shown in the OCT image).

Next, volumetric renderings of VET based off the segmented data were generated, and the 3D vaginal canal reconstruction of the natural menopause patient is presented in Figure 3. The reconstructions of VET from the four datasets demonstrated location dependency of the features and structures within the vaginal canal. The vaginal wall appeared to be a more level topography with thinner overall VET in the proximal region. The mid-section of the canal showed the transition from the proximal region to the distal region, where abundant vaginal folds exist, and VET was visibly thicker. In the distal opening of the 3D reconstruction, parts of the labia minora can be identified.

3.2 3D visualization of spatial-dependent VET changes

We demonstrated the representative VET distribution before and 4 – 6 weeks after the laser treatment for the two menopause patients: patient 1 and 2 in Table 1. Figure 4A&C shows the 3D reconstruction and the measurement of VET across the entire vaginal tract in patient 1, a 70-year-old patient with menopause due to natural aging process. From 3D VET model, there appears to be increased vaginal folds at distal part as indicated by the perturbing features in the reconstruction (pointed by the black arrows). The mean VET of the natural menopause patient showed significant increase, from 130 ± 26 μm to 181 ± 54 μm after the laser treatment ($p < 0.05$), which was more than one standard deviation of the baseline VET. Of further interest was the variation in VET along the vaginal length in the 70-year-old patient. Specifically, the proximal vagina was noted to have a thicker VET with

a clear transition point compared to the mid and distal vagina. After laser ablation, the mid and distal vagina demonstrated a greater change in VET.

Figure 4B&D shows the 3D reconstruction and the measurement of VET across the entire vaginal tract in patient 2, a 45-year-old patient with surgically induced menopause. Unlike the rest of the patients, the patient 2 is induced menopause and she has been wearing an estrogen ring during the laser treatment. We found the mean VET of the surgical menopause patient did not change significantly (from 296±36 μm to 293±36 μm, p=0.246). Overall, there were little noticeable changes in both 3D VET visualization as well as the VET changes for the patient 2.

3.2 Evaluation of laser effects on VET

To further investigate the effect of laser treatment on the vaginal thickness, we acquired OCT images from total of 12 patients and compared the VET before and after treatment (Table 1). Note that patient 2 was excluded from the evaluation of laser effects due to her medical history and age; estrogen ring, induced menopause, and her relatively young age can all potentially have an effect on the measurement. From each patient, mean VET in proximal and posterior vaginal tract were calculated. Among the rest of 11 patients, 6 patients showed increase in both proximal and posterior VET and 3 patients showed decrease in both proximal and posterior VET. 2 patients present mixed response where either proximal or posterior VET is increased. Interestingly, the patients with decreased thickness had thicker baseline VET, with more than 150 μm, while the patients with increased thickness generally had thinner baseline VET, with less than 150 μm. This indicate the vaginal epithelial changes in response to the laser can be highly dependent on the initial tissue histology.

4 DISCUSSIONS

While laser therapy has demonstrated clear benefits in areas of medicine such as dermatology, it remains an investigational therapy in female pelvic medicine as the body of literature on this topic evolves. Standardized protocols do not exist for the use of such devices and studies on treatment efficacy are inconclusive, warranting further investigation [9]. In this study, we investigated the clinical utility of intravaginal OCT endoscopy as a minimally invasive method to evaluate tissue-level response to the CO_2 laser ablation therapy. The OCT probe design enables capturing 3D structure of the entire vaginal canal, allowing for visualizing the longitudinal changes of vaginal microanatomy that provide insights into vaginal health. Since volumetric scanning yields hundreds of images per scan, we applied a deep learning segmentation algorithm for high-throughput analysis. As such, VET measurements can be speedily obtained during the patient's visit, and such quantitative patient-specific information may personalize the treatments for GSM symptoms as it can identify the regions within the vagina that require further or less intervention.

The capability of visualizing depth-resolve tissue microanatomy in the vagina, *in vivo*, allows for direct measures of morphological and pathophysiologic response to therapy. In the case of assessing laser therapy as presented in this study, our approach helps identify the regions that the laser ablation may be effective. This provides valuable feedbacks for optimizing energy-based devices for relieving GSM symptoms by fine-tuning parameters

such as duration, dosage, and frequency based on locations. With the ability to quantify vaginal tissue health, the utility of intravaginal OCT endoscope can be further extended to evaluating the efficacies of other types of interventions, such as topical estrogen, systemic hormone replacement therapy, or non-medicated topical moisturizers. At present, clinicians primarily collect feedback through patient-reported outcome measures. Gauging the response to therapy with quantifiable OCT measurements will provide an objective approach to screen patients that can benefit from the laser treatment, evaluate the treatment performance, aiding the development of new devices and pharmaceuticals.

Twelve postmenopausal patients undergoing CO_2 laser treatment were evaluated using OCT in this study (see Table 1), and all subjects reported little to no discomfort during the imaging. In our previous study, we showed that VET differs among premenopausal, perimenopausal, and postmenopausal women, with the postmenopausal category having the thinnest VET [30]. In this study we demonstrated both proximal and distal VET increased 1 month after the laser therapy in 6 out of 11 patients, supporting the previous clinical findings that laser ablation promoting epithelium proliferation in the vagina [34,35]. The findings demonstrate the efficacy of the proposed intravaginal OCT as a quantitative method for monitoring vaginal epithelium health, providing a platform for future pharmacological and medical device developments aiming to improve the quality of life among postmenopausal women.

In this study, 1.3 μm swept-source OCT system and oblong-shape catheter probe was implemented. However, different OCT configuration and source wavelength can be used depending on targeted gynecological features. For example, compared to standard OCT systems based on 1.3 μm wavelength laser, 1.7 μm OCT system has advantage of improved imaging depth due less tissue scattering. In vaginal tissue imaging, 1.7 μm system can potentially provide more details within lamina propria due to the extended light penetration depth [29,36]. However, in this study, our focus lies in accurately measuring the thickness of vaginal epithelial layer, which is typically less than 0.5 mm in thickness. Hence, both 1.3 μm and 1.7 μm imaging system can visualize epithelial layer. We implemented 1.3 μm OCT imaging system for this study as more off-the-shelf components are available. In addition, lower wavelength provide advantage in higher spatial resolution to assess the epithelium thickness more accurately. For instance, Duan et al. demonstrated colposcopic imaging based on visible-light OCT to archive ultra-high axial resolution of 2 μm [24]. However, visible-light OCT often requires additional calibration to achieve maximum performance as it is more susceptible to chromatic aberrations than near-infrared [37]. In addition to the source wavelength, different probe design can be considered in the future studies. We implemented rotational scanning probe to cover larger surface area during imaging. However, one possible limitations of this type of probe compared to raster scanning-based probe is the nonuniform rotation distortion (NURD) [38,39]. In proximal rotational scanning of OCT catheter probe, mechanical friction applied to imaging probe may induce NURD in the acquired images. In our case, bending of the outer plastic cover and the sheath during imaging can create friction. To alleviate the potential problems and the imaging artifacts associated with NURD, a straightforward approach is to carefully select the wall thickness and stiffness of the outer plastic cover to prevent any deformation in the oblong-shape cover. Some previous studies have also suggested to reduce NURD through distal rotational

scanning using micromotor catheters [40,41] or to correct the image distortion artifacts in post-processing [38,42,43]. In the future studies, we will investigate and compare different scanning schemes for obtaining clinically viable information while minimizing the imaging artifacts.

5 CONCLUSION

In this pilot study performed on 11 natural menopause patients, 6 patients showed increased VET after the laser treatment in both the proximal and distal vagina. 2 patients showed increase VET in either the proximal or distal vagina. Spatial distribution of VET observed using intravaginal OCT provides insights into laser micro-ablation treatment strategies, as it suggests the changes in the tissue is highly heterogeneous. Further investigation of light-based imaging of the capillaries net in the lamina propria, and elasticity of the vaginal wall may offer a new concept of scientific data about age-related changes, lubrication, and control of urination

ACKNOWLEDGMENTS

We thank Dr. Jiang Zhu for helping to develop the image acquisition device. We thank the individuals participated in the human study. Author 1 and Author 2 contributed equally to this work.

FINANCIAL DISCLOSURE

This study was supported by the National Institutes of Health (R01EB-030558, R01HL-125084, R01HL-127271, R01EY-026091, R01EB-030024), Air Force Office of Scientific Research (FA9550–20-1–0053), and the CounterACT Program, National Institutes of Health, Office of the Director, and the National Institute of Environmental Health Sciences (U54 ES027698) (CWW).

DATA AVAILABILITY STATEMENT

Research data are not shared.

Abbreviations:

GSM	Genitourinary syndrome of menopause
VET	vaginal epithelial thickness
PAI	Photoacoustic imaging
OCT	optical coherence tomography

REFERENCES

[1]. Mac Bride MB, Rhodes DJ, and Shuster LT, Mayo Clin. Proc. 2010, 85, 87. [PubMed: 20042564]

[2]. Portman DJ, Gass MLS, Kingsberg S, Archer D, Bachmann G, Burrows L, Freedman M, Goldstein A, Goldstein I, Heller D, Iglesia CB, Kagan R, Spadt SK, Krychman M, Nachtigall L, Nappi RE, Pinkerton JV, Shifren J, Simon J, and Stuenkel C, Menopause 2014, 21, 1063. [PubMed: 25160739]

[3]. Nappi RE and Palacios S, Climacteric 2014, 17, 3.

[4]. Santoro N and Komi J, J. Sex. Med. 2009, 6, 2133. [PubMed: 19493278]

[5]. Gandhi J, ; Chen Andrew, Dagur G, Suh Y, Smith N, Cali B, Sardar B, and Khan A, Am. J. Obstet. Gynecol. 2016, 215, 704. [PubMed: 27472999]

[6]. Cancelo-Hidalgo MJ and Coello LB, "Genitourinary Syndrome of the Menopause: Vaginal Health and Microbiota," in Menopause (Springer International Publishing), pp. 91–107

[7]. Rossouw JE, Anderson GL, Prentice RL, LaCroix AZ, Kooperberg C, Stefanick ML, Jackson RD, Beresford SAA, Howard BV, Johnson KC, Kotchen JM, and Ockene J, J. Am. Med. Assoc. 2002, 288, 321.

[8]. Anderson GL and Limacher M, J. Am. Med. Assoc. 2004, 291, 1701.

[9]. Tadir Y, Gaspar A, Lev-Sagie A, Alexiades M, Alinsod R, Bader A, Calligaro A, Elias JA, Gambaciani M, Gaviria JE, Iglesia CB, Selih-Martinec K, Mwesigwa PL, Ogrinc UB, Salvatore S, Scollo P, Zerbinati N, and Nelson JS, Lasers Surg. Med. 2017, 49, 137. [PubMed: 28220946]

[10]. Tadir Y, Iglesia C, Alexiades M, Davila GW, Guerette N, and Gaspar A, Lasers Surg. Med. 2019, 51, 315. [PubMed: 30408203]

[11]. Samuels JB and Garcia MA, Aesthetic Surg. J. 2019, 39, 83.

[12]. Sokol ER and Karram MM, Menopause 2017, 24, 810. [PubMed: 28169913]

[13]. Perino A, Calligaro A, Forlani F, Tiberio C, Cucinella G, Svelato A, Saitta S, and Calagna G, Maturitas 2015, 80, 296. [PubMed: 25596815]

[14]. Lee MS, Laser Ther. 2014, 23, 129. [PubMed: 25071312]

[15]. Balica A, Wald-Spielman D, Schertz K, Egan S, and Bachmann G, Maturitas 2017, 102, 69. [PubMed: 28610687]

[16]. Steinkampf MP, J. Reprod. Med. Obstet. Gynecol. 1988, 33, 931.

[17]. Qu Y, Li C, Shi J, Chen R, Xu S, Rafsanjani H, Maslov K, Krigman H, Garvey L, Hu P, Zhao P, Meyers K, Diveley E, Pizzella S, Muench L, Punyamurthy N, Goldstein N, Onwumere O, Alisio M, Meyenburg K, Maynard J, Helm K, Slaughter J, Barber S, Burger T, Kramer C, Chubiz J, Anderson M, McCarthy R, England SK, Macones GA, Zhou Q, Shung KK, Zou J, Stout MJ, Tuuli M, and Wang LV, J. Biomed. Opt. 2018, 23, 1.

[18]. Huang D, Swanson EA, Lin CP, Schuman JS, Stinson WG, Chang W, Hee MR, Flotte T, Gregory K, Puliafito CA, and al. et, Science 1991, 254, 1178. [PubMed: 1957169]

[19]. Fujimoto JG, Brezinski ME, Tearney GJ, Boppart SA, Bouma B, Hee MR, Southern JF, and Swanson EA, Nat. Med. 1995, 1, 970. [PubMed: 7585229]

[20]. Chuchuen O, Maher JR, Henderson MH, Desoto M, Rohan LC, Wax A, and Katz DF, PLoS One 2017, 12, e0185633. [PubMed: 28961280]

[21]. Wax A, Kashuba ADM, Katz DF, Maher JR, Henderson MH, Rinehart MT, Chuchuen O, and Kim S, Biomed. Opt. Express, Vol. 6, Issue 6, pp. 2022–2035 2015, 6, 2022. [PubMed: 26114026]

[22]. Drake TK, DeSoto MG, Peters JJ, Henderson MH, Murtha AP, Katz DF, and Wax A, Biomed. Opt. Express 2011, 2, 2850. [PubMed: 22025989]

[23]. Drake T, Peters J, Henderson M, DeSoto M, Katz D, and Wax A, Opt. Life Sci. 2011, paper OTuB5.

[24]. Duan L, McRaven MD, Liu W, Shu X, Hu J, Sun C, Veazey RS, Hope TJ, and Zhang HF, 10.1117/1.JBO.22.5.056003 2017, 22, 056003.

[25]. Xu L, Ma Q, Lin S, Ju J, Feng S, Shi Z, Bai Y, Song J, Du J, and Wang B, Sci. Reports 2022 121 2022, 12, 1.

[26]. Moiseev AA, Sirotkina MA, Potapov AL, Matveev LA, Vagapova NN, Kuznetsova IA, and Gladkova ND, J. Biophotonics 2021, 14, e202100055. [PubMed: 34057296]

[27]. Vincent KL, Vargas G, Wei J, Bourne N, and Motamedi M, Am. J. Obstet. Gynecol. 2013, 208, 282.e1. [PubMed: 23333551]

[28]. Vincent KL, Stanberry LR, Moench TR, Breitkopf CR, Loza ML, Wei J, Grady J, Paull J, Motamedi M, and Rosenthal SL, Obstet. Gynecol. 2011, 118, 1354. [PubMed: 22105265]

[29]. Li Y, Sudol NT, Miao Y, Jing JC, Zhu J, Lane F, and Chen Z, Lasers Surg. Med. 2019, 51, 120. [PubMed: 30058722]

[30]. Sudol NT, Miao Y, Li Y, Chen JJ, Jing JC, Zhu J, Tadir Y, Zhongping C, and Lane F, Female Pelvic Med. Reconstr. Surg. 2019, 26, 155.

[31]. Jing J, Zhang J, Loy AC, Wong BJF, and Chen Z, J. Biomed. Opt. 2012, 17, 110507. [PubMed: 23214170]

[32]. Ronneberger O, Fischer P, and Brox T, "U-net: Convolutional networks for biomedical image segmentation," in Lecture Notes in Computer Science (Including Subseries Lecture Notes in Artificial Intelligence and Lecture Notes in Bioinformatics) (Springer Verlag), 9351, pp. 234–241

[33]. del Amor R, Morales S, Colomer A, Mogensen M, Jensen M, Israelsen NM, Bang O, and Naranjo V, Front. Med. 2020, 7, 220.

[34]. Lapii GA, Yakovleva AY, Neimark AI, and Lushnikova EL, Bull. Exp. Biol. Med. 2017, 163, 280. [PubMed: 28726192]

[35]. Salvatore S, Nappi RE, Zerbinati N, Calligaro A, Ferrero S, Origoni M, Candiani M, and Leone Roberti Maggiore U, Climacteric 2014, 17, 363. [PubMed: 24605832]

[36]. Li Y, Jing J, Heidari E, Zhu J, Qu Y, and Chen Z, Sci. Rep. 2017, 7, 14525. [PubMed: 29109462]

[37]. Chong SP, Zhang T, Kho A, Bernucci MT, Dubra A, and Srinivasan VJ, Biomed. Opt. Express 2018, 9, 1477. [PubMed: 29675296]

[38]. Ahsen OO, Lee H-C, Giacomelli MG, Wang Z, Liang K, Tsai T-H, Potsaid B, Mashimo H, and Fujimoto JG, Opt. Lett. 2014, 39, 5973. [PubMed: 25361133]

[39]. Kang W, Wang H, Wang Z, Jenkins MW, Isenberg GA, Chak A, and Rollins AM, Opt. Express 2011, 19, 20722. [PubMed: 21997082]

[40]. Tran PH, Mukai DS, Brenner M, and Chen Z, Opt. Lett. 2004, 29, 1236. [PubMed: 15209258]

[41]. Jing JC, Chou L, Su E, Wong BJF, and Chen Z, Sci. Rep. 2016, 6, 39443. [PubMed: 27991580]

[42]. Miao Y, Jing JJ, and Chen Z, Biomed. Opt. Express 2021, 12, 2508. [PubMed: 33996244]

[43]. Mavadia-Shukla J, Zhang J, Li K, and Li X, J. Innov. Opt. Health Sci. 2020, 13, 2050030.

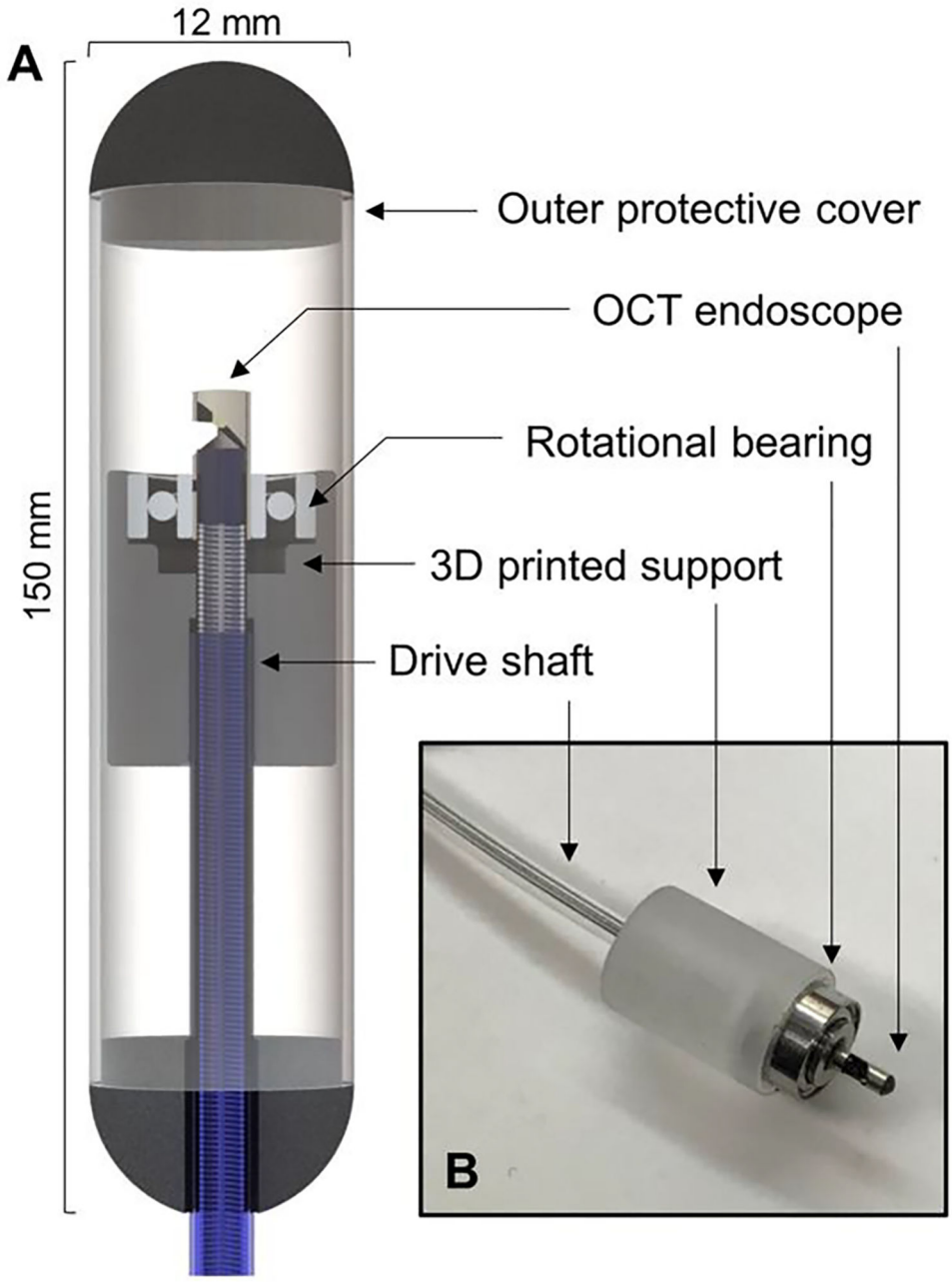

FIGURE 1.

[Handheld intravaginal OCT endoscope schematic. (A) 3D rendering of the intravaginal endoscope. (B) Centerpiece of the endoscope which provide helical scanning of the tissue. The rotation of the catheter-type endoscope is supported by a rotational bearing.]

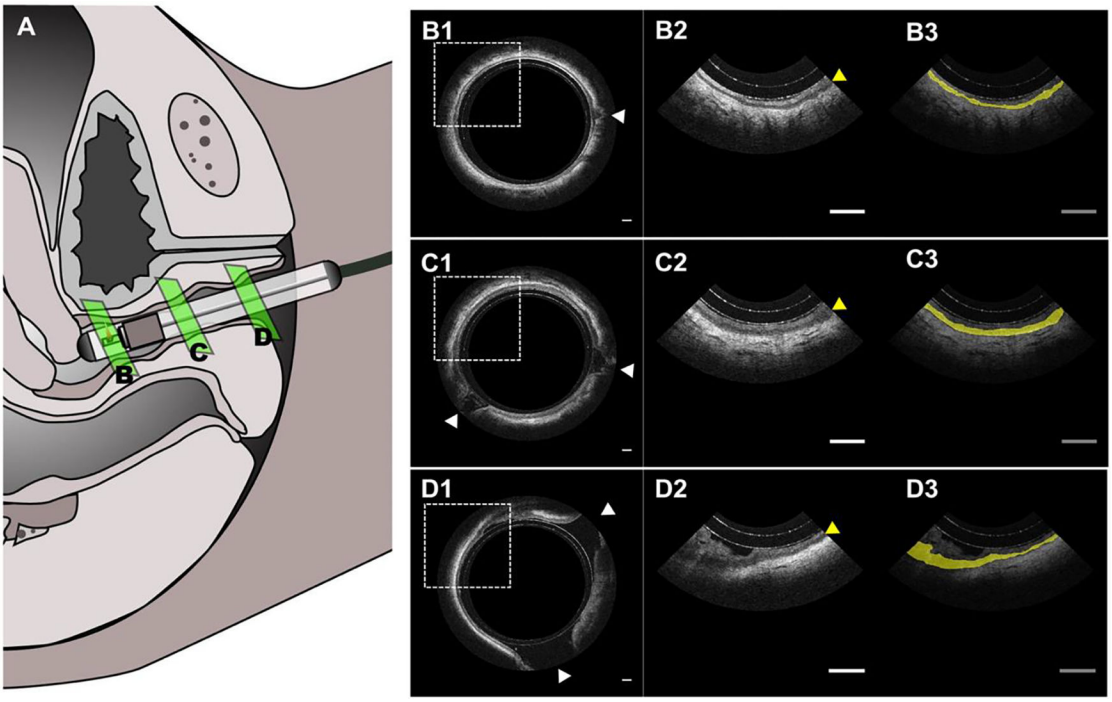

FIGURE 2.

[In vivo OCT imaging of a 70-year-old menopausal patient. (A) Schematic of in vivo human imaging and the placement of endoscope. (B) Intravaginal OCT endoscopy image of the proximal vagina near cervix with an expanded view (B2-D2) and the highlight of VEL (B3-D3). (C) OCT image acquire at proximal vagina. (D) OCT image acquired at distal vagina near the opening. The white arrows indicate vaginal folding and the yellow arrows indicate VEL. Scale bar: 1 mm.]

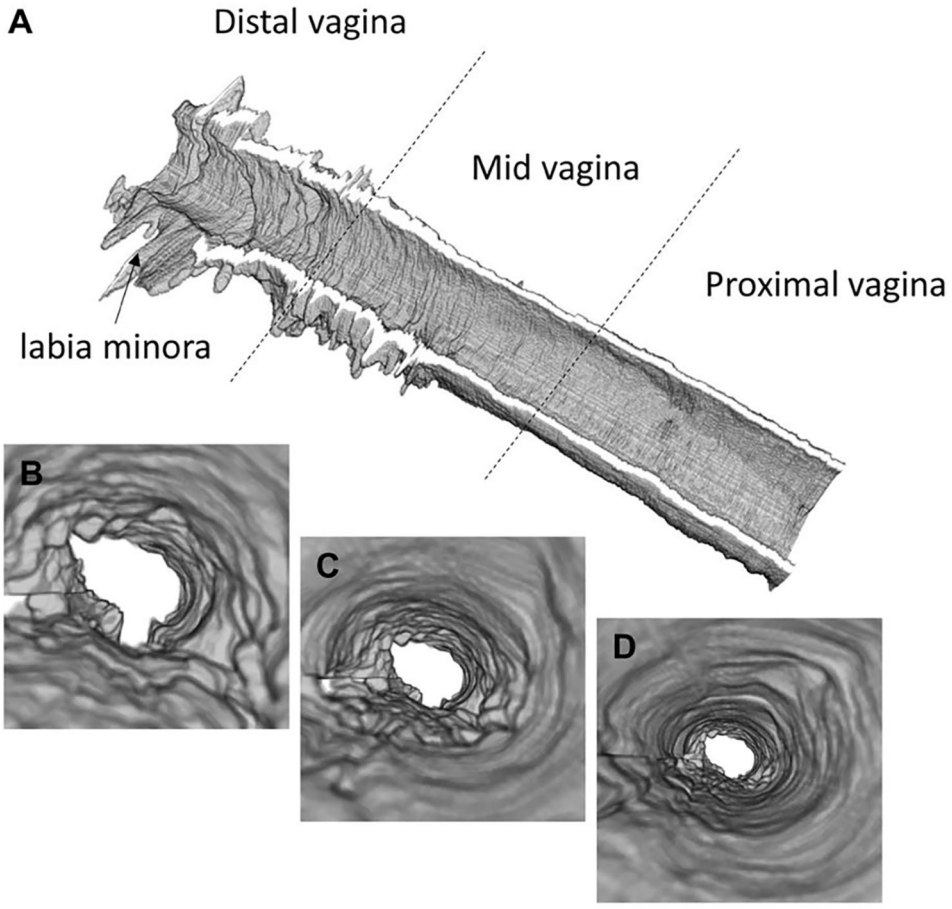

FIGURE 3.

[Three-dimensional reconstruction of vaginal epithelium. (A) 3D rendering of the entire vaginal canal showing the VEL thickness and surface topology of a menopausal patient. (B-D) flythrough views of VEL feature at proximal (B), mid (C), and distal (D) vagina.]

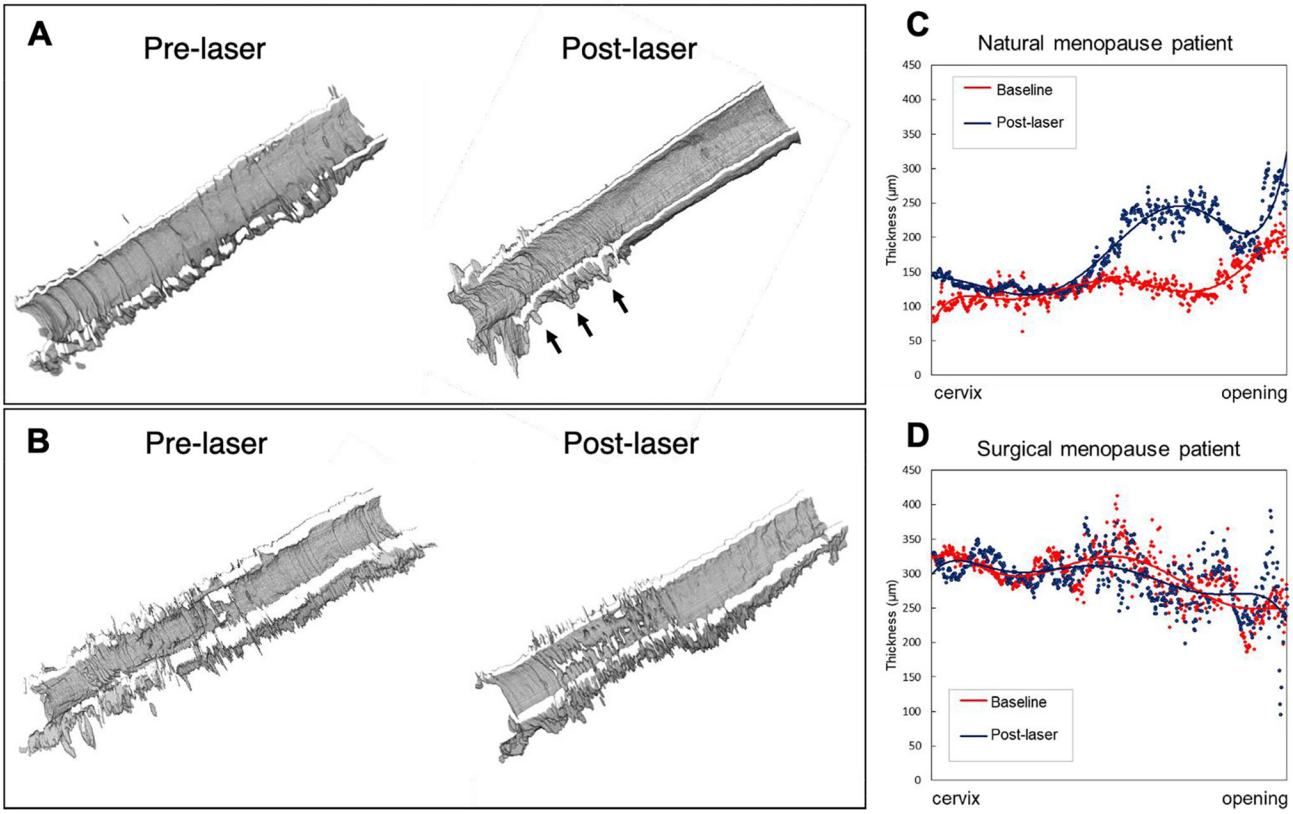

FIGURE 4.

[Morphological comparison of menopausal patients before and after laser. (A) Reconstruction of 70-year-old patient's VET with natural menopause. (B) Reconstruction of 40-year-old patient's VET with surgical menopause. (C and D) VET measured at different anatomical locations along the vaginal canal. The vertical axis indicates the thickness in um and the horizontal axis indicates the anatomical location.]

Table 1.

[Summary of VET changes before and 1-month after laser treatment in all menopause patients.

Case	Age	Baseline [um]		1 Month Post-laser [um]		ΔVET	
		Proximal	Posterior	Proximal	Posterior	Proximal	Posterior
1	70	97	144	145	229	▲ 47	▽ 85
2*	45	324	281	312	278	▽ 12	▽ 3
3	68	225	148	181	131	▽ 44	▽ 16
4	54	85	74	105	105	▲ 19	▲ 30
5	54	117	120	153	144	▲ 35	▲ 23
6	56	191	152	161	144	▽ 29	▽ 7
7	66	55	65	129	130	▲ 74	▲ 65
8	68	95	56	103	79	▲ 8	▲ 22
9	54	135	146	142	174	▲ 7	▲ 27
10	55	93	81	108	65	▲ 14	▽ 16
11	58	155	148	113	119	▽ 42	▽ 29
12	56	184	194	176	247	▽ 8	▲ 53

Note that patient 2 (indicated by *) is surgical menopause case and all other patients are natural menopause case.]